# Environmental Science
## Processes & Impacts

Accepted Manuscript


This article can be cited before page numbers have been issued, to do this please use: Y. Zeng, Z. Shen, Y. Lei, T. Zhang, Q. Zhang, H. Xu, Q. Wang, J. Cao and Y. Liu, *Environ. Sci.: Processes Impacts*, 2018, DOI: 10.1039/C8EM00144H.




ROYAL SOCIETY OF CHEMISTRY

rsc.li/process-impacts

View Article Online
DOI: 10.1039/C8EM00144H



Environmental Significance Statement

In this study, we investigated the factors controlling the distribution of ($PM_{2.5}$) Polycyclic aromatic hydrocarbons (PAHs) over Xi'an, China: uptake, affinity, removal mechanism. Source categories, partitioning behavior and chemical loss route were elucidated systematically to explore governing factor. Coal combustion, biomass burning, and vehicle emissions comprised the major PAH sources. Our results highlighted that the process of PAH partitioning was thermally controlled and component-dependent. Heterogeneous reaction with $NO_2$, OH, and $O_3$, as well as the aqueous reaction, effectively reduced $PM_{2.5}$ PAHs levels.

It is important to identify the decisive and influential factors of PAH distribution. This research provides a detailed insight into factors affecting $PM_{2.5}$ PAH distribution, as well as a theoretical basis for critical steps to control PAHs. Additionally, the knowledge of $PM_{2.5}$ PAHs governing factors can help to formulate an effective control scheme by the government.

View Article Online
DOI: 10.1039/C8EM00144H



# PAHs in fine particles over Xi'an, a typical northwestern city in China: sources, distribution, and controlling factors

Yaling Zeng[a,b], Zhenxing Shen[a,b], Yali Lei[a], Tian Zhang[a], Qian Zhang[a], Hongmei Xu[a], Qiyuan Wang[b], Junji Cao[b], Yang Liu[a]

[a]Department of Environmental Science and Engineering, Xi'an Jiaotong University, Xi'an 710049, China

[b] State Key Laboratory of Loess and Quaternary Geology, Institute of Earth Environment, Chinese Academy of Sciences

*Author to whom correspondence should be addressed. E-mail: zxshen@mail.xjtu.edu.cn (Zhenxing Shen)

View Article Online
DOI: 10.1039/C8EM00144H



**Abstract**: Levels of particle-bound polycyclic aromatic hydrocarbons (PAHs) are affected by emission as well as multiple factors. In this study, we investigated sources, uptake, affinity, and removal mechanism of PAHs in fine particles ($PM_{2.5}$). Source strength was analyzed with source apportionment, which was conducted by principal component analysis (PCA), positive matrix factorization (PMF) and diagnostic ratio. The octanol - air and soot-air partitioning model was used to elucidate the partitioning behavior of $PM_{2.5}$ PAHs. And chemical reactivity of $PM_{2.5}$ PAHs was analyzed to explain PAHs removal from particles. Coal combustion, biomass burning, and vehicle emissions comprised the major sources of PAHs. The process of partitioning was thermally controlled and component-dependent. Heterogeneous reaction with $NO_2$, OH, and $O_3$, as well as the aqueous reaction, effectively reduced $PM_{2.5}$ PAHs levels. The systematic analysis combined with field observations revealed that emission strength is the dominant factor controlling $PM_{2.5}$ PAH distribution. Source strength governed level of $PM_{2.5}$ PAHs though uptake, partitioning behavior and chemical removal kinetics, and peripheral imposing non-ignorable impact. Heterogeneous and aqueous reactions were the dominating mechanism of PAH removal from particles. This research provides a comprehensive insight into controlling factors on $PM_{2.5}$ PAH distribution in Xi'an, as well as a theoretical basis for critical steps to control PAH levels.

**Keywords**: Polycyclic aromatic hydrocarbons (PAHs); Source apportionment; Gas/particle partition; Principal component analysis (PCA); $K_{OA}$–$K_{SA}$ model

View Article Online
DOI: 10.1039/C8EM00144H



## 1. Introduction

Polycyclic aromatic hydrocarbons (PAHs) in fine particles ($PM_{2.5}$) have been of much interest to researchers [1, 2]. Some PAHs are well known as carcinogens, mutagens, and teratogens and therefore pose a serious threat to the human health and ecological balance [3, 4]. Multiple factors affect the PAH distribution in ambient $PM_{2.5}$[5]. Distinguishing the decisive and influential elements are necessary to alleviate PAHs pollution [6]. Identification of sources of PAHs in PM2.5 is a critical step for component and physicochemical character analysis [7]. Their basic types of sources are natural and anthropogenic, both of which can be subdivided [8]. Natural sources of PAHs include release by plants and combustion [9], while anthropogenic source are more complicated, including fossil fuel combustion, biomass burning, and industrial sources [10]. Identification of predominant sources of PAHs in ambient $PM_{2.5}$ and determining the relative contribution of each source may be done by source apportionment through mathematical analytical methods. Widely accepted and valid approaches are principal component analysis (PCA) [11] positive matrix factorization (PMF) [7], and chemical mass balance (CMB) [12].

PAHs in the atmosphere exist in two phases, namely, gaseous and particle phases [13]. Knowledge of the concentration distribution is necessary for adequate assessments of their potential health effects and environmental behavior [14]. The affinity of PAHs to particles in terms of the ability of capturing pollutant molecules and preventing release can be described by their partitioning behavior [13]. The earliest work on the partition process assumes that particles in the atmosphere are solid and that the uptake

View Article Online
DOI: 10.1039/C8EM00144H



of PAHs involves adsorption to a solid or solid-like surface [15, 16]. It has been subsequently recognized that many atmospheric particles are liquid or have liquid-like outer layers; hence, the uptake of gases can be treated as absorption by a liquid [15]. On the basis of these two fundamental transfer mechanisms, several models have been developed to elucidate the partition process. The Junge–Pankow model and the $K_{OA}$ absorption model are classical models that have been widely used for the partitioning behavior of atmospheric organic matter (OM) such as polychlorinated dibenzo-*p*-dioxins, dibenzofurans, dioxin-like polychlorinated biphenyls (PCBs) [17], and polybrominated diphenyl ethers (PBDEs) [7, 8]. Various lines of evidence from both laboratory and field studies indicate that the trend for the Junge–Pankow model fits better adsorption-dominated partition processes, while the $K_{OA}$-based model predictions have greater accuracy in absorptive partitioning [18, 8, 17]. The limitations of these two models lie in the difficulty of selecting the appropriate model without a clear determination of the partition pattern [18].

The reactions of particulate PAHs have been investigated for many years; both the reaction kinetics and the influencing factors have been explored [19]. Chemical loss through heterogeneous and aqueous reaction of particulate PAHs is evidenced by experimental and field studies [20]. Particle-bound PAHs are subject to various degradation processes, which may modify their physicochemical properties and decrease their concentration in particles [20]. The most important process is heterogeneous reaction initiated by various atmospheric oxidants ($NO_2$, OH, and $O_3$) [21]. Aqueous reactions can also partly explain PAHs loss [22]. PAH degradation through

View Article Online
DOI: 10.1039/C8EM00144H



heterogeneous and aqueous reaction accounted 30-100% loss in different interaction surroundings [23, 24]. Therefore, chemical loss through reaction played a non-negligible role in PAHs balance.

Xi'an, a typical inland city in northwestern China, has suffered particle pollution, especially during the winter [1, 2]. PAHs have maintained a high level over this city [1], thus increasing the health risk posed by $PM_{2.5}$. Factors that determine the concentrations of PAHs in $PM_{2.5}$ are important in ascertaining the fate of these carcinogens. At present, no appropriate comprehensive studies have elucidated the dominant elements of PAHs; this has hindered further understanding and control PAHs pollution. This paper discusses the source strength analysis and gas/particle partitioning behavior of PAHs over Xi'an, as well as their heterogeneous and aqueous reactions and the important factors of this process. We linked a source apportionment procedure and PCA with the Octanol–air partition and soot–air partition model ($K_{OA}$–$K_{SA}$model, which is a combination of two distinctive partition behaviors). A dataset for 81 $PM_{2.5}$ samples that were collected during the four seasons in 2015 was evaluated. Discussion on the weighting for each impact factor focuses on (a) the source strength analysis for carriers of $PM_{2.5}$ PAHs, as well as the (b) gas/particle partition behavior and (c) heterogeneous and aqueous reactions of PAHs.

## 2. Experiments and theoretical basis

### *2.1 Sample preparations*

The sampling site is located in a southeastern area of downtown Xi'an, which experiences heavy air pollution produced by surrounding residential areas, a school

View Article Online
DOI: 10.1039/C8EM00144H



campus, and major traffic roads [25]. The sampling site was located about 100 m from the South Second Ring Road in the southeastern part of downtown Xi'an (Fig. S1). To the north and east of the sampling site were residential areas and the Xi'an Jiaotong University (XJU) campus, while the South Second Ring road is to the south, and the Xingqin and Youyi Roads are to the west (as can be seen from Fig. S1). Ambient $PM_{2.5}$ aerosol samples were collected on pre-combusted quartz filters using a high-volume (~1.13 $m^3 \cdot min^{-1}$) air sampler (HVS-$PM_{2.5}$, Thermo-Anderson Inc.) at the rooftop of a 15 m high building. We collected 81 daily samples which reflected typical polluted weather in each season (24 h starting at 9:30 a.m.) from May 12 2015 to January 8 2016.

*2.2 Chemical analysis*

Each of the collected ambient filters was punched into a circular filter (diameter: ¼47mm) for PM chemical composition analysis. PAHs, levoglucose, organic carbon (OC), elemental carbon (EC), and water-soluble ions were separately determined by instrumental analysis.

Levoglucose and the 16 PAHs on the priority list, namely, (naphthalene (Nap), acenaphthylene (Acy), acenaphthene (Acp), fluorene (Flu), phenanthrene (Phe), anthracene (Ant), fluoranthene (Fl), pyrene (Pyr), benzo[*a*]anthracene (BaA), chrysene (Chr), benzo[*b*]fluoranthene (BbF), benzo[*k*]fluoranthene (BkF), benzo[*a*]pyrene (BaP), indeno[1,2,3-*cd*]pyrene (Ind), dibenzo[*a*,*h*]anthracene (Di(a,h)A), and benzo[*g*,*h*,*i*]perylene (B(g,h,i)P)), were analyzed using gas chromatography with mass selective detection (7890, Agilent, USA). Samples were analyzed for 16 PAHs and levoglucosan by extracting the analytes into dichloromethane (DCM) - methanol solvent (1:1) using ultrasonic agitation after the addition of deuterated PAH surrogate

View Article Online
DOI: 10.1039/C8EM00144H



standards which was repeated three times. The organic extracts were combined and the solvent was removed using a rotary evaporator. Interfering compounds were removed by homemade silicon seizuring (alumina: silica gel: Anhydrous sodium sulfate =3:2:1). This was followed by rotary evaporation until approximately 1–2 ml volume and filtered. Then, under a gentle stream of nitrogen, the samples were reduced almost to dryness and redissolved with n-hexane. Internal standard hexamethylbenzene was added and the volume was adjusted to 1 ml. PAHs were directly analyzed and levoglucosan was silanization to analyze using gas chromatography with mass selective detection (GC/MS). The chromatographic conditions were as follows: injector temperature 290 °C and detector temperature 250 °C. The temperature ramp was an initial oven temperature of 50 °C maintained for 2 min, increased at 5 °C/min to280°C, and then increased at 3°C to a maximum of 300 °C for 10 min. The detection limit, recovery, and standard deviation (SD) were listed in Table S1.

Three quarters of each circle filter were dissolved into distilled deionized water (10, 2.0, and 15 mL) with a resistivity of 18.3 MU for separate analysis of water-soluble ions. Each solvent was sonicated for 1 h and shaken by mechanical shaker for 1 h, and kept at room temperature for 20 h allowing the solution reaching equilibrium. All the extracts were filtered 1~3 times with a 0.45 mm pore size microporous membrane, and then stored at 4□ in a clean tube until sample analysis. The concentrations of extracts ($NO_3^-$, and $SO_4^{2-}$) were analyzed using an ion chromatography (IC, Dionex 500, Dionex Corp, Sunnyvale, California, United States). The detection limit was 0.002 mgL-1for levoglucosan. Quality control data was seen in Table S1.

For thermal carbonaceous analysis (OC and EC), a 0.5 $cm^2$ punch of each sample was analyzed using a DRI Model 2001 Thermal and Optical Carbon Analyzer (Atmoslytic Inc., Calabasas, CA, USA) following the IMPROVE TOR protocol [26, 27]. Four OC fractions (OC1, OC2, OC3, and OC4 at 140 C, 280 C, 480 C, and 580 C, respectively, in a non-oxidizing helium atmosphere), and three EC fractions (EC1,

View Article Online
DOI: 10.1039/C8EM00144H



EC2, and EC3 at 580 C, 740 C, and 840 C, respectively, in a 2% oxygen/98% helium atmosphere) were produced. During volatilization of organic carbon, part of organic carbon was converted pyrolytically to EC (this fraction of OC was named as OP) [27]. Hence, the IMPROVE protocol defines OC as OC1+OC2+OC3+OC4+OP and EC as EC1+EC2+EC3- OP. And Table S1 listed detection limit, recovery, SD of OE/EC determination.

*2.3 Partition theory*

It is common to express the extent of sorption as ($F$/TSP)/$A$, where $F$ and $A$ (ng·m$^{-3}$) are the particle-associated and gaseous concentrations, respectively, and TSP (μg·m$^{-3}$) is the total suspended particulate matter concentration [28]. In this study, PAHs, OC, and EC in the $PM_{2.5}$ were characterized [29]. The partition coefficient in this work was defined as follows:

$$K_P = K_{PM2.5} = \frac{Pticulate_{2.5}/PM_{2.5}}{Gas} \quad \text{..... (1)}$$

The fractions of OC and EC were defined as follows:

$$f_{OC} = f_{OC,2.5} = \frac{OC_{2.5}}{PM_{2.5}} \quad \text{..... (2)}$$

$$f_{EC} = f_{EC,2.5} = \frac{EC_{2.5}}{PM_{2.5}} \quad \text{..... (3)}$$

where $PM_{2.5}$, $OC_{2.5}$, and $EC_{2.5}$ are the measured concentrations of $PM_{2.5}$, OC, and EC, respectively. Dachs et al 2004 assumed that EC accounts for most of soot carbon, and that there is no difference between soot and EC. Henry's law constant is required to estimate $K_{SA}$. This constant gives the ratio between gaseous and dissolved concentrations in equilibrium. EC and octanol were used to model the soot carbon in adsorptive partitioning and OM in absorptive partitioning, respectively. The overall gas–particle partition coefficient that accounts for both the OM and the soot phases for

View Article Online
DOI: 10.1039/C8EM00144H



both absorptive and adsorptive partitioning is given by Eq. (4). We assumed that $a_{EC}/a_{AC} = 1$, $f_{OM} = 1.6f_{TOC}$, and $f_{OC}/f_{EC} = 3$ (Odabasi et al., 2006).

$$K_P = \frac{f_{OM} MW_{OCT} \zeta_{OCT} K_{OA}}{\rho_{OCT} MW_{OM} \zeta_{OM} 10^{12}} + \frac{f_{EC} a_{EC} K_{SA}}{a_{AC} 10^{12}} \quad \text{(4)}$$

where $f_{TOC}$ is the fraction of total organic carbon, $\rho oc_T$ is 0.820 kg·L$^{-1}$, $f_{TOC}$ is the fraction of total organic carbon, $\zeta_{OCT}$ is the activity coefficient of the absorbing compound in octanol, $\zeta_{OM}$ is the activity coefficient of the compound in the OM phase, $f_{EC}$ is the fraction of EC in the aerosol, $a_{EC}$ is the specific surface areas of EC (62.7 m$^2$·g$^{-1}$), $a_{AC}$ is the specific surface area of activated carbon, and $K_{SA}$ is the soot–air partition coefficient.

$K_{OA}$ and $P_L^0$ are related through the following equation [30]:

$$K_{OA} = \frac{C_O}{C_A} = \frac{RT}{\zeta_{OCT} V_{OCT} P_L^0} \quad \text{(5)}$$

where $C_O$ and $C_A$ are the equilibrium concentrations (mol·m$^{-3}$) of the solute in octanol and air, respectively. $R$ is the universal gas constant (8.314 Pa·m$^{-3}$·mol$^{-1}$·K$^{-1}$), $T$ is temperature (K), ζoct is the activity coefficient in octanol, $V_{OCT}$ is the molar volume of octanol ($1.58 \times 10^{-4}$ m$^3$·mol$^{-1}$), and $P_L^0$ is the supercooled-liquid vapor pressure (Pa). $\zeta_{OCT}$ was determined by using a regression equation for PAHs ($r^2$ = 0.999, $n$ = 13) soluble in octanol [28]. A good and nearly 1:1 relationship between log $K_{OA}$ and log$P_L^0$ was obtained. Calculated $\zeta_{OCT}$ values for PAHs range between 3.2 and 6.2, indicating near-ideal solution behavior.

$$\log K_{OA} = -0.97 \log P_L + 6.65 \quad \text{(6)}$$

Dachs et al [31] proposed a theory, the $K_{OA}$–$K_{SA}$ model, which takes into account both adsorption on EC and OC in $PM_{2.5}$. Jordi Dachs et al [32] suggested that the

View Article Online
DOI: 10.1039/C8EM00144H



thermodynamics-based model reported by Noort et al [33] can be used to estimate $K_{SA}$ for PAHs, which is a function of supercooled-liquid vapor pressure ($P_L^0$, Pa) and EC specific surface area ($\alpha_{EC}$, $m^2 \cdot g^{-1}$), $P_L^0$, a function of temperature, was calculated using Eq. (7):

$$\log K_{SA} = -0.85 \log P_L^0 + 8.94 - \log \frac{998}{a_{EC}} \quad (7)$$

$a_{EC}$ (62.7 $m^2 \cdot g^{-1}$) was taken from a recent study by Jonker et al [34]:

$$\log K_{SA} = -0.85 \log P_L^0 + 7.74 \quad (8)$$

Eqs. (6) and (8) were used in Eq. (4) to obtain the final formula:

$$K_P = \frac{1}{10^{12}} \left( f_{OM} 9.72 * 10^{-0.97\left(\frac{c}{T}+b\right)+6.65} + f_{EC} 10^{-0.85\left(\frac{c}{T}+b\right)+7.74} \right) \quad (9)$$

Eq. (9) quantitatively expresses $K_P$ as a function of ambient temperature, chemical composition, and supercooled liquid vapor pressure, which was determined from the molecular weights and structures of the PAHs [35].

*2.4 Source apportionment model*

Source categories for $PM_{2.5}$ from Xi'an were identified by PCA using SPSS 18.0 software. PCA is an effective tool for identifying independent factors using the eigenvector decomposition of a matrix of pairwise correlations among compound concentrations [9]. Principal component analysis is a linear transformation that decorrelates multivariate data by translating the axes of the original feature space. Therefore, the data can be represented as a new component space without correlation [11].

In this study, PCA with varimax normalized rotation was performed. Each factor from PCA was associated with source characterizations by its most representative source markers. There were 81 samples and 13 markers, meeting the model calculation

View Article Online
DOI: 10.1039/C8EM00144H



accuracy that $N > 30 + (V + 3)/2$ (where $N$ = number of samples and $V$ = number of variables) [36].

## 3. Results and discussion

### *3.1 Levels and Source apportionment of $PM_{2.5}$*

The level $PM_{2.5}$ and PAHs in Xi'an was demonstrated in Fig.1. The level of ∑PAH was 28.45~167.98 ng/m$^3$ and the average was 75.29 ± 23.39 ng/m$^3$ which was lower than previous study by Shen et al [1] with $PM_{2.5}$ ranged from 130 to 404.1μg/m$^3$. This centration was agree well with Xu et al [2] who demonstrated that 16 PAHs concentrations in Xi'an ranged from 32.4 to 104.7 ng /m$^3$, with an average value of 57.1 ± 23.0 ng/ m$^3$.

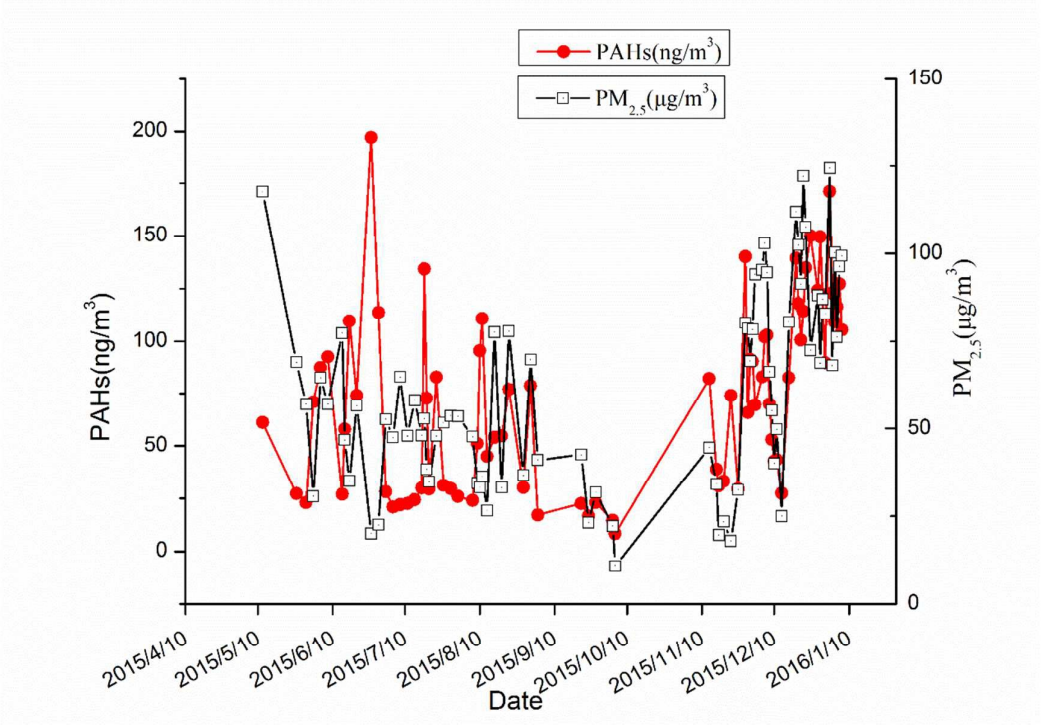


Fig. 1 Levels of $PM_{2.5}$ and PAHs in Xi'an

Source strength analysis, which was conducted by source apportionment in this research, was a significant part. This method identifies the important surrogate sources

View Article Online
DOI: 10.1039/C8EM00144H



using the PCA technique and Kaiser's criteria [37]. Here, the eigenvalue of impact factors is greater than 1 and reaches an inflection in the scree plot (Fig. S2). By using this method, we established four principal sources (Factors 1–4), which accounted for 77.5% of $PM_{2.5}$ sources.

Table 1 lists the principal component loadings, which indicate the correlations of each variable with factors, and source contribution analysis of $PM_{2.5}$ was shown in Fig.2. Factor 1 is responsible for 32.82% of the total variance and is highly correlated with high-ring PAHs which are accepted markers of coal combustion (CC) [38]. The diagnostic ratio of Bap/BghiP=2.74 (>0.9) verified contribution of coal combustion [39]. Factor 2 is responsible for 23.71%of the total variance. This factor is predominantly composed of OC, EC, and levoglucose, which are typically attributed to biomass burning (BB); from this finding, we judged Factor 2 as the BB source [40]. The third factor is responsible for 12.75 % of the total variance. The low-ring PAHs Phe and Pyr usually originate from gasoline and diesel combustion[41, 42]; from this, Factor 3 was judged as vehicular emission (VE). The fourth factor is responsible for 6% of the total variance. Factor 4 was recognized as secondary organic carbon (SOC) because of the dependence of SOC the markers $NO_3^-$ and $SO_4^{2-}$ [43].

Table 1 Component matrix

| Components | Factors | | | |
|---|---|---|---|---|
| | 1 | 2 | 3 | 4 |
| Phe | 0.48 | -0.38 | 0.68 | 0.10 |
| Ant | 0.74 | -0.38 | 0.14 | -0.11 |
| Fl | 0.87 | 0.01 | -0.35 | -0.11 |
| Pyr | 0.50 | -0.31 | 0.59 | -0.21 |
| BaA | 0.84 | 0.07 | -0.51 | 0.08 |
| Chr | 0.75 | 0.29 | 0.12 | -0.23 |
| Ind | 0.82 | -0.01 | -0.46 | 0.19 |
| BghiP | 0.68 | 0.00 | 0.34 | 0.20 |
| OC | 0.10 | 0.94 | 0.18 | -0.11 |
| EC | 0.09 | 0.94 | 0.18 | -0.06 |
| NO3- | 0.18 | 0.13 | 0.10 | 0.71 |

View Article Online
DOI: 10.1039/C8EM00144H

| | | | | |
|---|---|---|---|---|
| SO42- | 0.23 | -0.06 | 0.10 | 0.58 |
| levoglucosan | 0.15 | 0.91 | 0.15 | 0.10 |

Diagnostic ratios of PAHs were conducted to make source identification, which can compare with the PCA and PMF analysis. Calculated PAH ratios of Ant/ (Ant+ Phe) was 0.4, which indicated biomass and coal combustion [44]. Bap/BghiP averaged 2.7 in this study, which implied contribution of coal combustion [39]. Additionally, Ind/ (Ind +BghiP) ratio in this study (0.5) indicated the source of coal combustion [45]. Flt/(Flt+Pyr) ratio (0.4) revealed the important contribution of fuel combustion [46]. Source identifications by diagnostic ratios of PAHs were consistent with PCA and PMF results as above description. The results indicated that the primary sources of PAHs in Xi'an were pyrogenic sources which include combustion of fossil fuel (coal and petroleum) and biomass.

The major $PM_{2.5}$ contributor composition is similar to the investigations by Wang et al. [47] in Xi'an. The epically CC, which is CC pollution still dominated in Xi'an and was thus the main contributor of PAHs [48]. Notably, OC and EC were abundant, and BB was the second largest source of $PM_{2.5}$. The particle mixture was partly composed of VE from vehicles in the metropolis. SOC was a small portion of $PM_{2.5}$, but they had an important effect on physicochemical properties [49]. Because markers for residential components showed minimal correlations, we do not further discuss them in this paper.

View Article Online
DOI: 10.1039/C8EM00144H



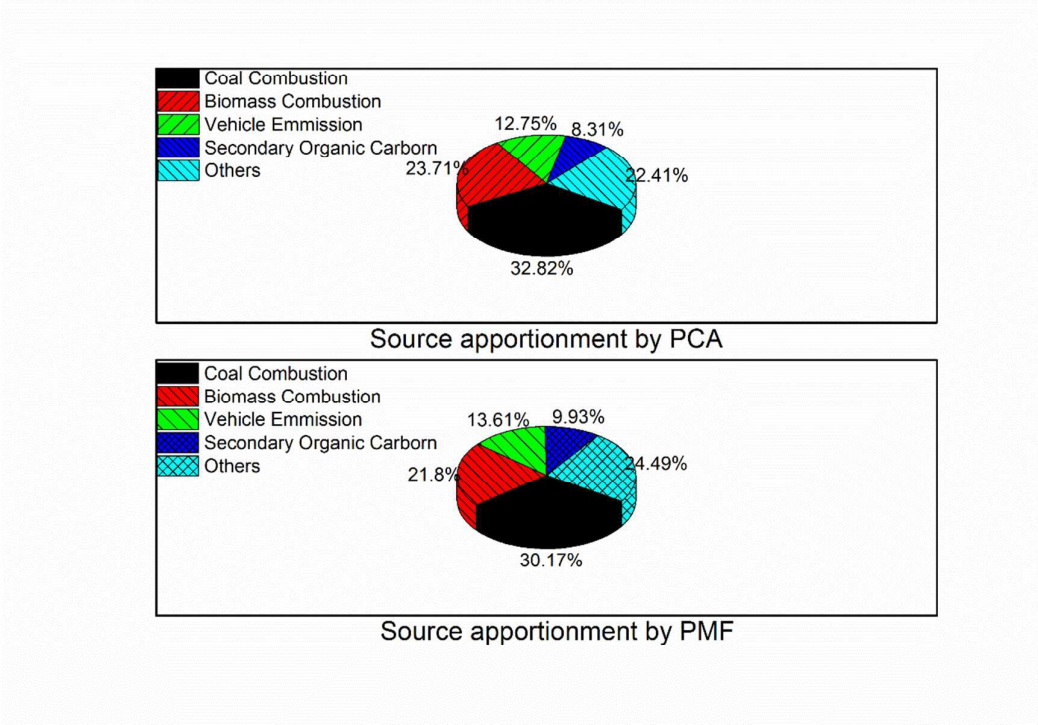


Fig.2 Source contribution analysis of $PM_{2.5}$

Evidently, anthropogenic combustion was the major source of $PM_{2.5}$ in Xi'an. $PM_{2.5}$ PAHs trend to originate from same source; hence, we can conclude that the pollutant originated from anthropogenic pyrolysis. PAHs from the four identified and one unrecognized source showed strong correlation with CC, BB, and VE. It is worth noting that OC and EC are abundant in BB, which have strong affinity to PAHs, consequently, BB should be an important source to PAHs. CC was the most prominent contributor of PAHs, but its affinity to PAHs was not significant as that of BB because of the lower levels of OM and EC.

*3.2 Evaluation of gas–particle distribution of PAHs by $K_P$*

$K_{OA}$ is the ratio of solute concentration in octanol to the concentration in air [15]. The $K_{OA}$ model used the external factors and the particle properties to describe the specific

View Article Online
DOI: 10.1039/C8EM00144H



partition behavior. Its hypothesis specifies OM as a coating layer over the aerosol particle. The absorption process depicted by the $K_{SA}$ model describes the interaction of OC with soot. Soot particles are the byproducts of the combustion of liquid and gaseous fuels, and their production depends strongly on the ratio of carbon to oxygen during combustion [49]. PAHs form concurrently with soot particles and play an important role in soot formation and particle growth [50]. Furthermore, PAHs have a high affinity to black carbon and activated carbon, as evidenced by adsorption experiments and theoretical predictions [51]. Therefore, the adsorption of PAHs onto the soot fraction or primary OC may be an important mechanism affecting the gas–particle partitioning of PAHs. There is good agreement between the measured partition ratio with $K_{OA}$–$K_{SA}$ model predictions [13]; the model thus describes well the transition and fate of PAHs. This model can be used to elaborate the partition behavior of PAHs in $PM_{2.5}$.

The supercooled-liquid vapor pressure ($P_L^0$), which can be determined from gas chromatographic retention times, was linearly correlated with $K_P$ according to the different partition models [28]. The method is reliable; it has been applied to the $P_L^0$ determination for many semi-volatile substances such as PCB, PBDE, and PAHs [52]. The $\log P_L^0$ value was correlated with $1/T$ over the environmental temperature range and showed a log linear relationship according to the equation,

$$\log P_L^0 = m_L(T,K)^{-1} + b_L \quad \text{.....(10)}$$

where $m_L$ and $b_L$ are regression parameters specific to each PAH [28]. Literature values for the coefficient ratio are dependent on both temperature and the number of carbon atoms; these literature data (Table S2) were used in the construction of the calibration

View Article Online
DOI: 10.1039/C8EM00144H



curve.

Accordingly, $K_P$ was thermally dependent; $K_P$ of PAHs decreased when the temperature rose since $K_P$ was inversely correlated with $\log P_L^0$. High $K_P$ values decreased sharply with the increase in temperature, while the low $K_P$ values changed more gently. The order of magnitude of the change ranged from 1 to 3; therefore, the ambient temperature had a notable impact on the gas and particle partitioning process. In the summer, PAHs in the atmosphere tend to be gaseous; in the winter, the pollutants tend to exist as particles. We set $f_{OM}$ and $f_{EC}$ as their average values, 0.35 and 0.10 which were determined in 81 samples, respectively and drew the trend line for the PAHs (Fig. 3).

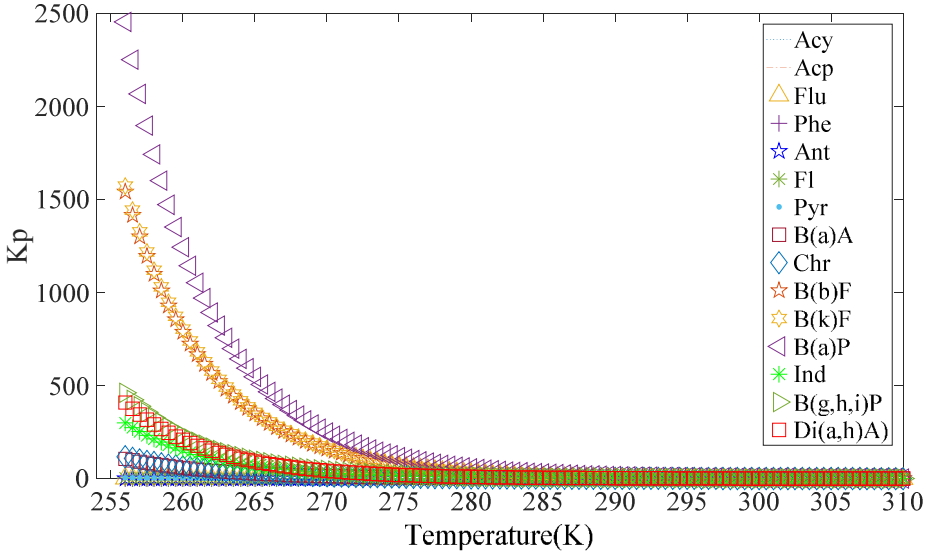


Fig. 3 Temperature dependence of $K_P$

The $K_{OA}$–$K_{SA}$ model describes adsorption onto particle surfaces and absorption onto aerosol OM as two proposed mechanisms [31]. Eq. (4) explicitly expresses both the

View Article Online
DOI: 10.1039/C8EM00144H



properties of the surface and those of the adsorbing SOC, which determine on a molecular level the amount of adsorption of the gas on the surface; hence, both absorptive and adsorptive partitioning were evident.

Fig. S3 illustrates the trend of $K_P$ for $PM_{2.5}$ concentrations during sampling events, which reflect $f_{OM}$ and $f_{EC}$ variations. The average ambient temperature of the four seasons in 2015 was chosen to confine thermodynamic characteristics: 291 K for spring, 300 K for summer, 288 K for autumn, and 278 K for winter. There was an overall increase in $K_P$ with the increase in $f_{OM}$ and $f_{EC}$ of $PM_{2.5}$, especially for OM, which tended to contribute greatly to the absorptive capacity. This mechanism (Fig. S3) implies that $K_P$ rises more sharply when the OM fraction increases more as compared with the EC fraction. Alternatively, the proportion of EC change affected the partitioning ability, although through a different mechanism. The trend of $K_P$ was related to the temperature, following the order winter > autumn > spring > summer. Notably, PAHs with higher molecular weight (HMW) or ring numbers were more strongly absorbed than those with lower weight molecular (LMW) and fewer rings, as expected. This results kept well with the findings by Wei et al.[53] in Xi'an who observed that LMW, and HMW accounted for 99% and 30% of the total gaseous plus particulate phases in March, and 99% and 46% in September.

The OM/EC ratio for certain aerosol particles is under statistical regulations [54]. In this study, we set $f_{TOC} = 4.98f_{EC}$, $f_{OC} = 3.98f_{EC}$ on average, and $f_{OM} = 7.968f_{EC}$, which were based on laboratory results. Subsequently, we depicted the change in trend with the ambient temperature and the $PM_{2.5}$ chemical composition (Fig. 4). This change

View Article Online
DOI: 10.1039/C8EM00144H



illustrates that high-ring PAHs at lower temperature and higher EC concentration tend to partition into particles. Comparisons for partitioning in the literature showed that low-ring PAHs in the atmosphere are gaseous and high-ring PAHs are particulate; these results agree well with recent field measurements by Callén et al[36]. The dependence of $K_P$ on temperature-sensitive chemical components is supported by studies conducted by other groups[13, 14].

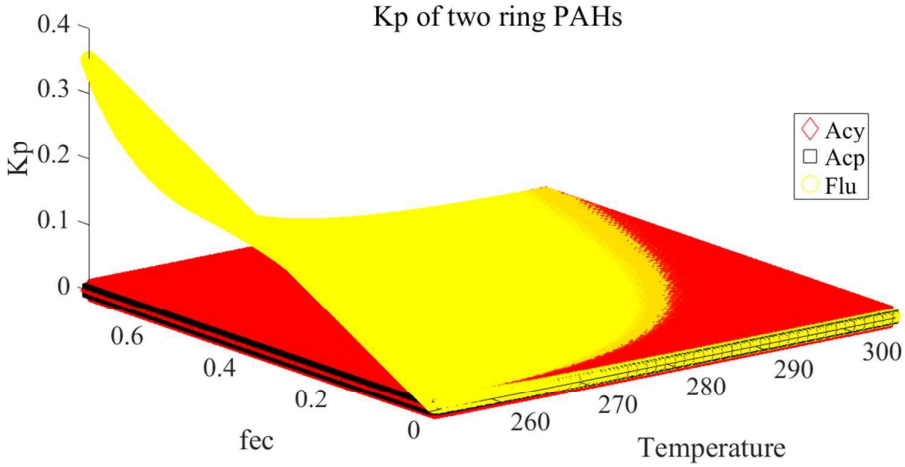

View Article Online
DOI: 10.1039/C8EM00144H



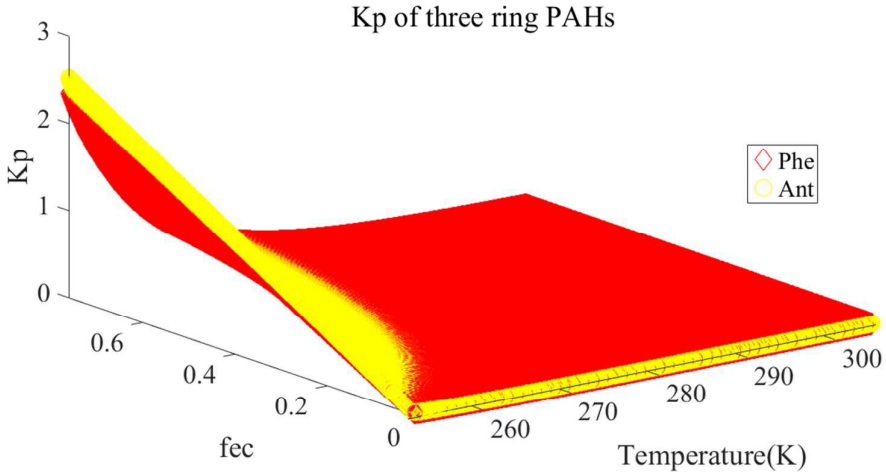


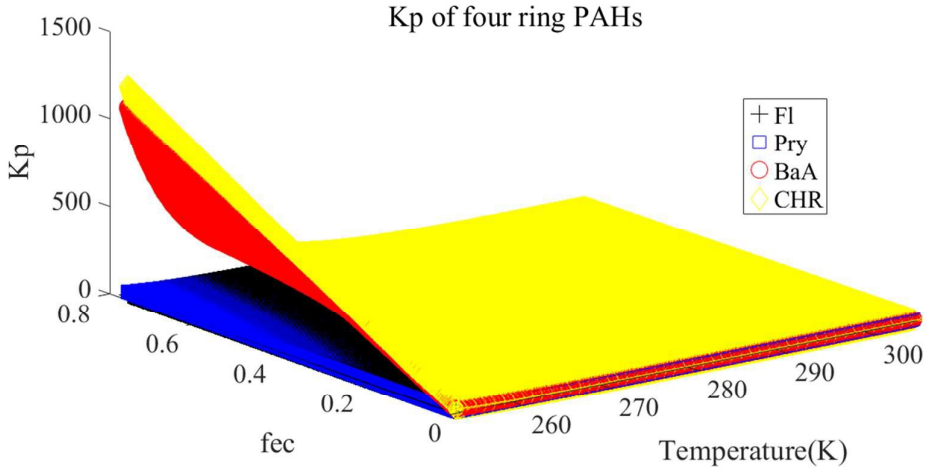

View Article Online
DOI: 10.1039/C8EM00144H



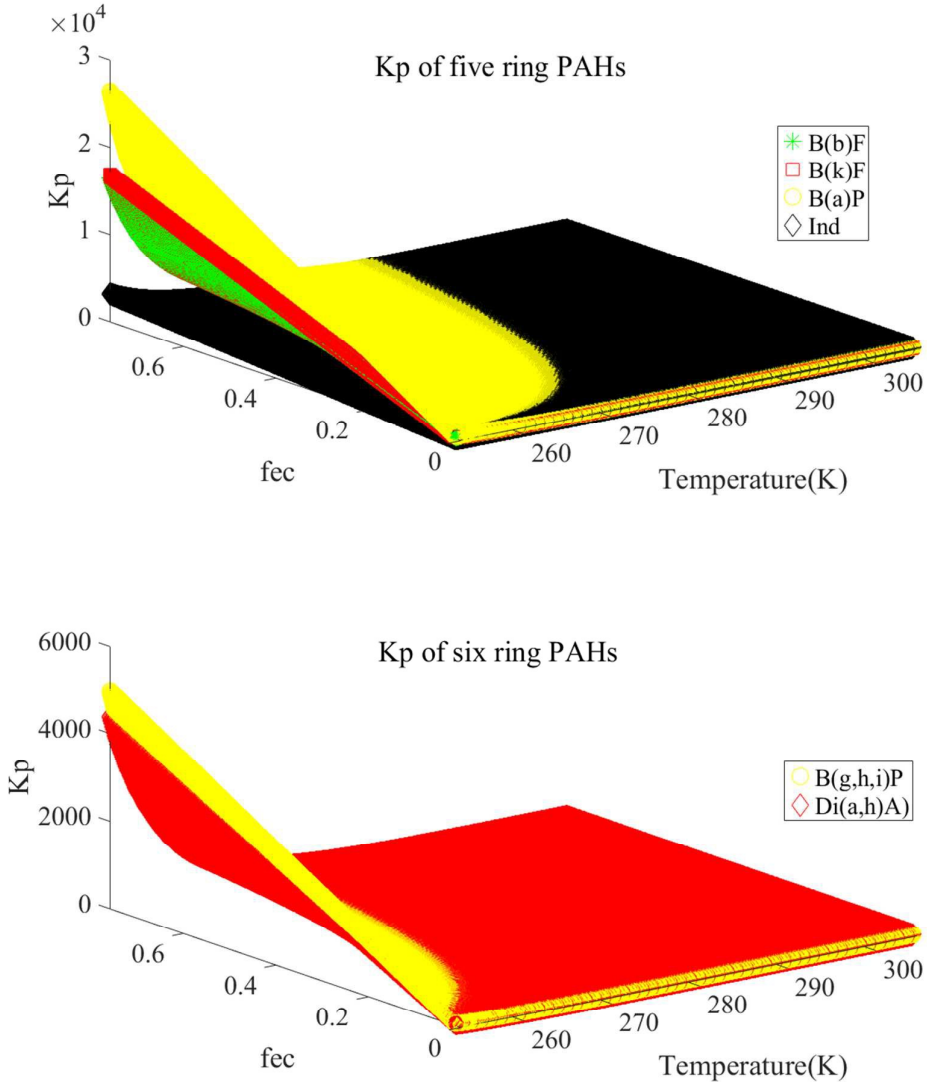


Fig. 4 Thermal and chemical composition dependence of *K*p

### *3.3 Chemical transformation of $PM_{2.5}$ PAHs*

Pseudo-first-order rate constants [55] were all on the same order of magnitude, falling within the range of (2.0–8.4) × $10^{-3}$ $s^{-1}$ at an initial $NO_2$ concentration of 8.0 × $10^{13}$ $cm^{-3}$·$molecule^{-1}$·$s^{-1}$. Ant, Pyr, BaP, and perylene were the PAHs that were most reactive to $NO_2$, whereas, BkF, Flu, and BaA showed the lowest reactivity to $NO_2$ [21].

View Article Online
DOI: 10.1039/C8EM00144H



The rate constants for the reaction with OH at an initial OH concentration of 3.4 × $10^{10}$ $cm^{-3}$·$molecule^{-1}$·$s^{-1}$ vary between 0.11 $s^{-1}$ (for Flu and Pyr) and 0.20 $s^{-1}$ (for B(g,h,i)P) [20]. Pseudo-first-order rate constants relative to the heterogeneous reaction of OH radicals with PAHs adsorbed on graphite particles were 0.11–0.2 $s^{-1}$. The rate for the reaction of $O_3$ with Ant on phenylsiloxane oil aerosols was 0.010 ± 0.003 $s^{-1}$, while that for the reaction on azelaic acid aerosols was 0.057 ± 0.009 $s^{-1}$ [55]. The rate of BaP reaction with $O_3$ was 0.015 ± 0.001 $s^{-1}$ on soot, while it was 0.048 ± 0.008 $s^{-1}$ on azelaic acid [56]. These rate constants confirm that the OH heterogeneous reaction is the process contributing to atmospheric loss of PAHs that dominates over reactions with $NO_2$ and $O_3$ [20, 22].

Dissolving PAHs in a prepared solvent and then photolyzing them under controlled condition is the general method for exploring aqueous reactions [57]. Pseudo-first-order rate constants for 16 PAHs were determined by monitoring the decrease in PAHs fluorescence intensity over time [57]. Pseudo-first-order rates ranged from $10^{-6}$ to $10^{-3}$, covering three orders of magnitude. Rates for low-ring PAHs were two orders of magnitude smaller than those for high-ring PAHs because of poor partitioning of low-molecular-weight PAHs in particles [20].

The temperature dependence of heterogeneous and aqueous reactions was another factor governing PAH distribution. The Arrhenius expression was used to describe the temperature dependence of the reaction [58]. Its frequently used form is

$$r = BT^{n}e^{-E_a/RT}$$

where $R$ is the gas constant, $T$ is the temperature in kelvins, and $E_a$ is the activation

View Article Online
DOI: 10.1039/C8EM00144H



energy, parameters that are characteristic of a particular reaction. *B* is a temperature-independent constant characteristic of the reaction, and *n* is the number that is adjusted to provide a best fit to the data. Most reactions in atmospheric chemistry studies increase in rate as the temperature increases [59, 60]. The temperature of Xi'an changed from −17 to 43°C during the sampling period, thereby expanding the difference in the reaction rate.

Total oxidant levels (OX; defined as $O_3$ + $NO_2$) were used as an index to measure atmospheric oxidizability [61]. The levels of $O_3$, $NO_2$, and OX in Xi'an for four seasons are summarized in Fig. 5. The OX concentration reached a peak in both summer and winter, with the peak in winter being higher that in the summer. The change in proportion of the two oxidants, namely, >80% contribution of $NO_2$ to OX in December and only less than 20% in July, and vice versa for $O_3$ concentration, explain this phenomenon. A similar seasonal trend for oxidation of PAHs was observed in the former study by Wang et al. [62]. The amount of OX in the atmosphere was related to reaction processes and was therefore linked to the conversion of PAHs[61].

The diurnal and seasonal variations of the OH radical concentration in the middle atmosphere can be observed[63]. The OH level in summer was much higher than that in winter, as has been observed by many researchers[64,65]. From the pseudo-first-order rate and the temporal distribution of OX, we can conclude that the transformation of PAHs in summer were more violent than they were in the winter.

View Article Online
DOI: 10.1039/C8EM00144H



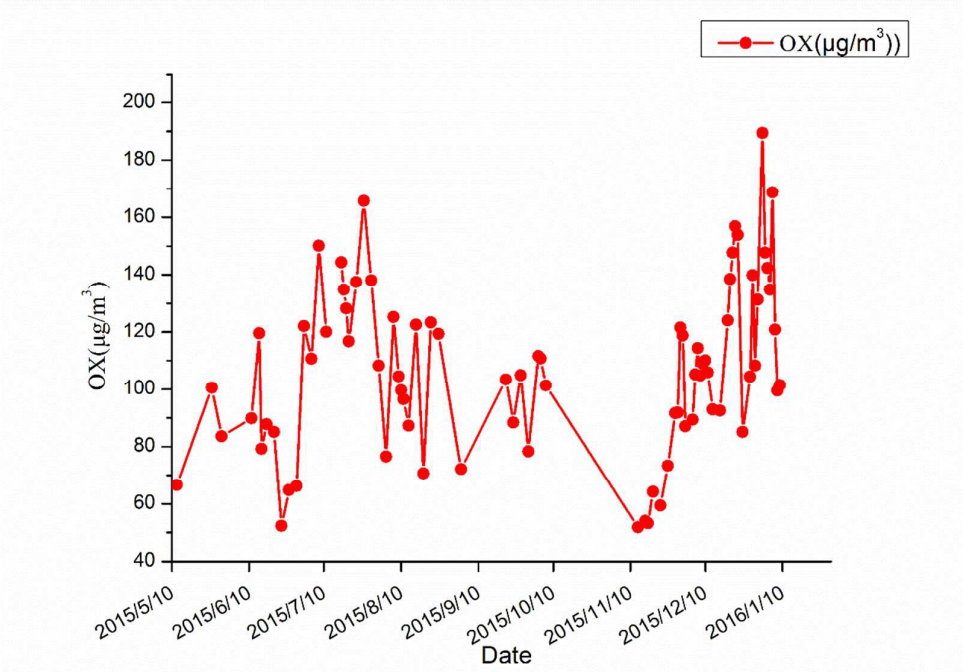


Fig. 5 Concentration of OX in Xi'an

Some experiments performed for certain periods (from minutes to hours) showed that the reactions reached a plateau[20]. According to the observation, the residues did not react regardless of the exposure time during the approach to the plateau. This observation with heterogeneous reactions has been made for all studied PAHs. The values for the plateaus reached 54%, 72%, 35%, and 38% for Ant, Pyr, BaP, and perylene, respectively[21]. PAHs processing in the atmospheric aqueous phase is considered to be less significant as that in the gas-phase and heterogeneous reactions [66]. However, aqueous reactions contribute to PAHs loss from aerosol particles. The rate of the OH reaction in the troposphere[66] or in hot and humid environments [64] may be significant. The first-order reaction rates for the reaction of the different PAHs with various oxidants thus vary beyond an order of magnitude[67].

View Article Online
DOI: 10.1039/C8EM00144H



*3.4 The factors that govern PAH distribution*

The percentage of PAH partitioning into particles according to the $K_{OA}$–$K_{SA}$ model can be seen in Fig. 6. The overall trend was that particle partitioning in the autumn and winter were greater than that in the spring and summer. The fractions of volatile Acy and Acp in particles were not higher than 0.0065 even in the coldest ambient condition of the investigated period. The semi-volatile PAHs were more sensitive to molecular weight, temperature, $f_{EC}$, and $f_{OM}$, and their ratios fluctuated with time. $K_P$ for five to six rings remained stable throughout the research period; the majority of PAHs were in the condensed phase except at three points in the summer, which lack OM and EC.

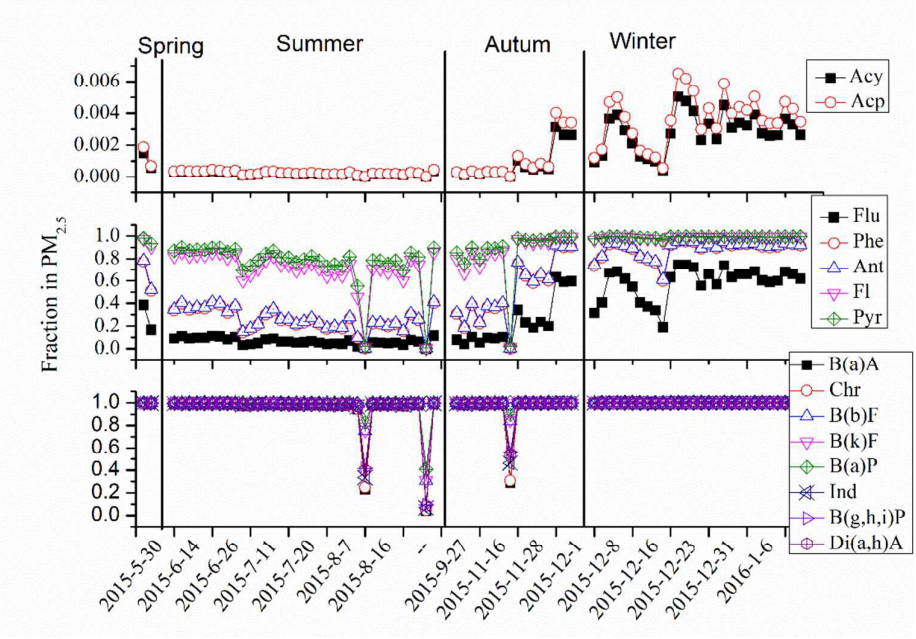


Fig. 6 PAHs fractions in $PM_{2.5}$ and seasonal variation

Fig. 7 illustrates the levels of PAHs during the research period, with the sub-graphs sorted according to volatility. The vast majority of PAHs could be detected in of the summer in Xi'an. However, Ant and Di (a,h)A were not subsequently detected

View Article Online
DOI: 10.1039/C8EM00144H



in $PM_{2.5}$ at high $K_P$. Clearly, the concentrations of PAHs were not positively correlated with their $K_P$ value. Volatile Acp tended to have high affinity to particles, but its determined concentration was higher especially in the winter. The $K_P$ for Ant was not the lowest among the semi-volatile PAHs, but its concentration was the lowest. Non-volatile PAHs had similar high $K_P$ values, but the differences in concentrations among PAHs were large. For example, Di(a,h)A was nearly undetectable in the four seasons but had high $K_P$. In addition, BaP had the strongest affinity to particles, but its concentration was not the highest among the non-volatile PAHs.

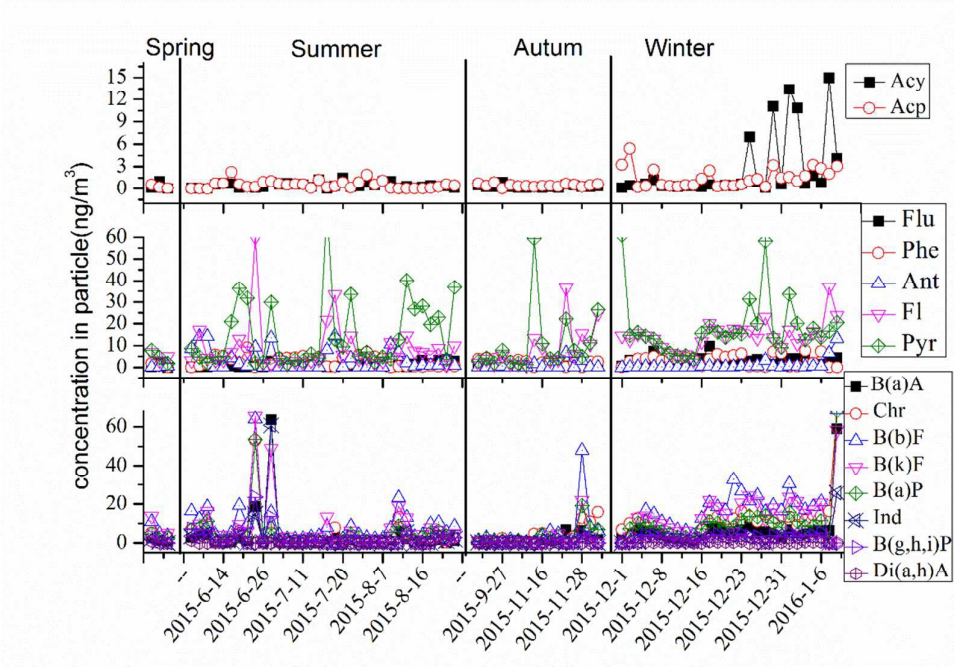


Fig. 7 Concentration of particle-bound PAHs

The effect of heterogeneous and aqueous reactions, which are vital to the chemical removal method, plays a changing role in the distribution of $PM_{2.5}$ PAHs. A high temperature increases the removal rate, whereas winter temperature hinders the reaction.

View Article Online
DOI: 10.1039/C8EM00144H



Comparing $PM_{2.5}$, Kp and OX level which reflected in Fig 1, 4 and 5, clearly, the PAHs level kept greater accordance with $PM_{2.5}$. Consequently, the correlations with source strength were greater than partitioning process and heterogeneous reaction. Therefore, particle-bound PAHs were influenced by source strength, $K_P$, and the reactivity in the atmosphere. The concentrations and the partition theory suggest that the emission strength and physicochemical property are the decisive factors. $K_P$, as well as heterogeneous and aqueous reactions, had a significant effect on the concentration distribution, and gaseous PAHs hardly converted to particles.

## 4. Conclusions

This study investigated the factors that controlled level of $PM_{2.5}$ PAHs over Xi'an. Results of sources apportionment indicated CC, BB, and VE accounted for an overwhelming fraction of $PM_{2.5}$, while CC was the dominant contributor of PAHs. Gas-particle partition process was more sensitive to temperature change than component variations, and its value decided by the PAH molecular weight and structure. Heterogeneous and aqueous reactions removed particle-bound PAHs effectively when surrounded with abundant oxidants. The level of $PM_{2.5}$ PAHs preferentially associated with source rather than peripheral condition. Hence, we can conclude that source strength is the dominant factor controlling the distributions of a majority of PAHs in Xi'an. This study offers a corroborating theory for the fate of PAHs and pollution abatement.

View Article Online
DOI: 10.1039/C8EM00144H



## Acknowledgements

This research was supported by the Natural Science Foundation of Shaanxi Province, China (2016ZDJC-22), National Natural Science Foundation of China (41573101), and State Key Laboratory of Loess and Quaternary Geology, Institute of Earth Environment, CAS (SKLLQG1616).

## References

1. Z. Shen, J. Cao, Z. Tong, S. Liu, L. Reddy, Y. Han, T. Zhang and J. Zhou, Chemical Characteristics of Submicron Particles in Winter in Xi'an, *Aerosol Air Qual. Res.*, 2009, **9**, 80-93.
2. H. Xu, S. Ho, M. Gao, J. Cao, B. Guinot, K. Ho, X. Long, J. Wang, Z. Shen, S. Liu, C. Zheng and Q. Zhang, Microscale spatial distribution and health assessment of $PM_{2.5}$-bound polycyclic aromatic hydrocarbons (PAHs) at nine communities in Xi'an, China, *Environ. Pollut.*, 2016, **218**, 1065-1073.
3. K. Kim, S. Jahan, E. Kabir and R. Brown, A review of airborne polycyclic aromatic hydrocarbons (PAHs) and their human health effects, *Environ. Int.*, 2013, **60**, 71-80.
4. J. Neff, S. Stout and D. Gunster, Ecological Risk Assessment of Polycyclic Aromatic Hydrocarbons in Sediments: Identifying Sources and Ecological Hazard, *Integr. Environ. Asses.*, 2005, **1**, 22-33.
5. P. Pandey, D. Patel, A. Khan, S. Barman, R. Murthy and G. Kisku, Temporal distribution of fine particulates ($PM_{2.5}$, $PM_{10}$), potentially toxic metals, PAHs and Metal-bound carcinogenic risk in the population of Lucknow City, India, *J. Environ. Sci. Heal. A*, 2013, **48**, 730-745.
6. K. Arzayus, R. Dickhut and E. Canuel, Fate of atmospherically deposited polycyclic aromatic hydrocarbons (PAHs) in Chesapeake Bay, *Environ. Sci. Technol.*, 2001, **35**, 2178-2183.

View Article Online
DOI: 10.1039/C8EM00144H



7. M. Callen, A. Iturmendi and J. Lopez, Source apportionment of atmospheric $PM_{2.5}$-bound polycyclic aromatic hydrocarbons by a PMF receptor model. Assessment of potential risk for human health, *Environ. Pollut.*, 2014, **195**, 167-177.
8. B. Gugamsetty, H. Wei, C. Liu, A. Awasthi, S. Hsu, C. Tsai, G. Roam, Y. Wu and C. Chen, Source Characterization and Apportionment of $PM_{10}$, $PM_{2.5}$ and $PM_{0.1}$ by Using Positive Matrix Factorization, *Aerosol Air Qual. Res.*, 2012, **12**, 476-491.
9. D. Wu, Z. Wang, J. Chen, S. Kong, X. Fu, H. Deng, G. Shao and G. Wu, Polycyclic aromatic hydrocarbons (PAHs) in atmospheric $PM_{2.5}$ and $PM_{10}$ at a coal-based industrial city: Implication for PAH control at industrial agglomeration regions, China, *Atmos. Res.*, 2014, **149**, 217-229.
10. B. Liu, J. Yang, J. Yuan, J. Wang, Q. Dai, T. Li, X. Bi, Y. Feng, Z. Xiao, Y. Zhang and H. Xu, Source apportionment of atmospheric pollutants based on the online data by using PMF and ME2 models at a megacity, China, *Atmos. Res.*, 2017, **185**, 22-31.
11. R. Lasaponara, On the use of principal component analysis (PCA) for evaluating interannual vegetation anomalies from SPOT/VEGETATION NDVI temporal series, *Ecol. Model.*, 2006, **194**, 429-434.
12. A. Villalobos, F. Barraza, H. Jorquera and J. Schauer, Wood burning pollution in southern Chile: $PM_{2.5}$ source apportionment using CMB and molecular markers, *Environ. Pollut.*, 2017, **225**, 514-523.
13. E. Demircioglu, A. Sofuoglu and M. Odabasi, Atmospheric Concentrations and Phase Partitioning of Polycyclic Aromatic Hydrocarbons in Izmir, Turkey, *Clean-Soil Air Water*, 2011, **39**, 319-327.
14. J. Parnis, D. Mackay and T. Harner, Temperature dependence of Henry's law constants and K-OA for simple and heteroatom-substituted PAHs by COSMO-RS, *Atmos. Environ.*, 2015, **110**, 27-35.
15. T. Harner and T. Bidleman, Measurement of octanol-air partition coefficients for

View Article Online
DOI: 10.1039/C8EM00144H



polycyclic aromatic hydrocarbons and polychlorinated naphthalenes, *J. Chem. Eng. Data*, 1998, **43**, 40-46.

16. J. Pankow, An Absorption-model of gas-particle partitioningof organic-compounds in the atmosphere, *Atmos. Environ.*, 1994, **28**, 185-188.
17. Q. Die, Z. Nie, F. Liu, Y. Tian, Y. Fang, H. Gao, S. Tian, J. He and Q. Huang, Seasonal variations in atmospheric concentrations and gas-particle partitioning of PCDD/Fs and dioxin-like PCBs around industrial sites in Shanghai, China, *Atmos. Environ.*, 2015, **119**, 220-227.
18. E. Perraudin, H. Budzinski and E. Villenave, Kinetic study of the reactions of $NO_2$ with polycyclic aromatic hydrocarbons adsorbed on silica particles, *Atmos. Environ.*, 2005, **39**, 6557-6567.
19. L. Zhu, X. Shi, Y. Sun, Q. Zhang and W. Wang, The growth mechanism of polycyclic aromatic hydrocarbons from the reactions of anthracene and phenanthrene with cyclopentadienyl and indenyl, *Chemosphere*, 2017, **189**, 265-276.
20. W. Esteve, H. Budzinski and E. Villenave, Relative rate constants for the heterogeneous reactions of $NO_2$ and OH radicals with polycyclic aromatic hydrocarbons adsorbed on carbonaceous particles. Part 2: PAHs adsorbed on diesel particulate exhaust SRM 1650a, *Atmos. Environ.*, 2006, **40**, 201-211.
21. W. Esteve, H. Budzinski and E. Villenave, Relative rate constants for the heterogeneous reactions of OH, $NO_2$ and NO radicals with polycyclic aromatic hydrocarbons adsorbed on carbonaceous particles. Part 1: PAHs adsorbed on 1-2 mu m calibrated graphite particles, *Atmos. Environ.*, 2004, **38**, 6063-6072.
22. J. Eagar, B. Ervens and P. Herckes, Impact of partitioning and oxidative processing of PAH in fogs and clouds on atmospheric lifetimes of PAH, *Atmos. Environ.*, 2017, **160**, 132-141.
23. E. Perraudin, H. Budzinski and E. Villenave, Kinetic study of the reactions of ozone with polycyclic aromatic hydrocarbons adsorbed on atmospheric model particles, *J. Atmos. Chem.*, 2007, **56**, 57-82.

View Article Online
DOI: 10.1039/C8EM00144H



24. C. Liu, P. Zhang, B. Yang, Y. Wang and J. Shu, Kinetic Studies of Heterogeneous Reactions of Polycyclic Aromatic Hydrocarbon Aerosols with NO3 Radicals, *Environ. Sci. Technol.*, 2012, **46**, 7575-7580.

25. Z. Shen, L. Zhang, J. Cao, J. Tian, L. Liu, G. Wang, Z. Zhao, X. Wang, R. Zhang and S. Liu, Chemical composition, sources, and deposition fluxes of water-soluble inorganic ions obtained from precipitation chemistry measurements collected at an urban site in northwest China, *J. Environ. Monit.*, 2012, **14**, 3000-3008.

26. J. Chow, J. Watson, D. Ono and C. Mathai, PM10 standards and nontraditional particulate source controls - a summary of the a-and-WMA/EPA international speacialty conference, *J. Air Waste Manage.*, 1993, **43**, 74-84.

27. J. Chow, J. Watson, L. Chen, W. Arnott, H. Moosmuller and K. Fung, Equivalence of elemental carbon by thermal/optical reflectance and transmittance with different temperature protocols, *Environ. Sci. Technol.*, 2004, **38**, 4414-4422.

28. M. Odabasi, E. Cetin and A. Sofuoglu, Determination of octanol-air partition coefficients and supercooled liquid vapor pressures of PAHs as a function of temperature: Application to gas-particle partitioning in an urban atmosphere, *Atmos. Environ.*, 2006, **40**, 6615-6625.

29. Y. Naumova, S. Eisenreich, B. Turpin, C. Weisel, M. Morandi, S. Colome, L. Totten, T. Stock, A. Winer, S. Alimokhtari, J. Kwon, D. Shendell, J. Jones, S. Maberti and S. Wall, Polycyclic aromatic hydrocarbons in the indoor and outdoor air of three cities in the US, *Environ. Sci. Technol.*, 2002, **36**, 2552-2559.

30. T. Harner and M. Shoeib, Measurements of octanol-air partition coefficients (K-OA) for polybrominated diphenyl ethers (PBDEs): Predicting partitioning in the environment, *J. Chem. Eng. Data*, 2002, **47**, 228-232.

31. J. Dachs and S. Eisenreich, Adsorption onto aerosol soot carbon dominates gas-particle partitioning of polycyclic aromatic hydrocarbons, *Environ. Sci. Technol.*, 2000, **34**, 3690-3697.

32. J. Dachs, S. Ribes, B. van Drooge, J. Grimalt, S. Eisenreich and O. Gustafsson, Response to the comment on "Influence of soot carbon on the soil-air partitioning

View Article Online
DOI: 10.1039/C8EM00144H



of polycyclic aromatic hydrocarbons", *Environ. Sci. Technol.*, 2004, **38**, 1624-1625.

33. P. van Noort, A thermodynamics-based estimation model for adsorption of organic compounds by carbonaceous materials in environmental sorbents, *Environ. Toxicol. Chem.*, 2003, **22**, 1179-1188.
34. M. Jonker and A. Koelmans, Sorption of polycyclic aromatic hydrocarbons and polychlorinated biphenyls to soot and soot-like materials in the aqueous environment mechanistic considerations, *Environ. Sci. Technol.*, 2002, **36**, 3725-3734.
35. Y. Lei, R. Chankalal, A. Chan and F. Wania, Supercooled liquid vapor pressures of the polycyclic aromatic hydrocarbons, *J. Chem. Eng. Data*, 2002, **47**, 801-806.
36. M. Callen, M. de la Cruz, J. Lopez, M. Navarro and A. Mastral, Comparison of receptor models for source apportionment of the PM10 in Zaragoza (Spain), *Chemosphere*, 2009, **76**, 1120-1129.
37. B. Williams, A. Onsman and T. Brown, Australian paramedic graduate attributes: a pilot study using exploratory factor analysis, *Emerg. Med. J.*, 2010, **27**, 794-799.
38. Y. Chen, G. Sheng, X. Bi, Y. Feng, B. Mai and J. Fu, Emission factors for carbonaceous particles and polycyclic aromatic hydrocarbons from residential coal combustion in China, *Environ. Sci. Technol.*, 2005, **39**, 1861-1867.
39. S. Peng, W. Wu and J. Chen, Removal of PAHs with surfactant-enhanced soil washing: Influencing factors and removal effectiveness, *Chemosphere*, 2011, **82**, 1173-1177.
40. X. Zhang, A. Hecobian, M. Zheng, N. Frank and R. Weber, Biomass burning impact on $PM_{2.5}$ over the southeastern US during 2007: integrating chemically speciated FRM filter measurements, MODIS fire counts and PMF analysis, *Atmos. Chem. Phys.*, 2010, **10**, 6839-6853.
41. J. Baker and M. Calvert, A study of the characteristics of slotted laminar jet diffusion flames in the presence-of non-uniform magnetic fields, *Combust. Flame*,

View Article Online
DOI: 10.1039/C8EM00144H



2003, **133**, 345-357.

42. A. Robinson, R. Subramanian, N. Donahue, A. Bernardo-Bricker and W. Rogge, Source apportionment of molecular markers and organic aerosols-1. Polycyclic aromatic hydrocarbons and methodology for data visualization, *Environ. Sci. Technol.*, 2006, **40**, 7803-7810.
43. X. Zhang, J. Wang, Y. Wang, H. Liu, J. Sun and Y. Zhang, Changes in chemical components of aerosol particles in different haze regions in China from 2006 to 2013 and contribution of meteorological factors the, *Atmos. Chem. Phys.*, 2015, **15**, 12935-12952.
44. A. Kamal, A. Cincinelli, T. Martellini, I. Palchetti, F. Bettazzi and R. Malik, Health and carcinogenic risk evaluation for cohorts exposed to PAHs in petrochemical workplaces in Rawalpindi city (Pakistan), *Int. J. Environ. Heal. R.*, 2016, **26**, 37-57.
45. E. Galarneau, Source specificity and atmospheric processing of airborne PAHs: Implications for source apportionment, *Atmos. Environ.*, 2008, **42**, 8139-8149.
46. M. Yunker, R. Macdonald, R. Vingarzan, R. Mitchell, D. Goyette and S. Sylvestre, PAHs in the Fraser River basin: a critical appraisal of PAH ratios as indicators of PAH source and composition, *Org. Geochem.*, 2002, **33**, 489-515.
47. J. Wang, S. Ho, R. Huang, M. Gao, S. Liu, S. Zhao, J. Cao, G. Wang, Z. Shen and Y. Han, Characterization of parent and oxygenated-polycyclic aromatic hydrocarbons (PAHs) in Xi'an, China during heating period: An investigation of spatial distribution and transformation, *Chemosphere*, 2016, **159**, 367-377.
48. T. Okuda, K. Okamoto, S. Tanaka, Z. Shen, Y. Han and Z. Huo, Measurement and source identification of polycyclic aromatic hydrocarbons (PAHs) in the aerosol in Xi'an, China, by using automated column chromatography and applying positive matrix factorization (PMF), *Sci. Total Environ.*, 2010, **408**, 1909-1914.
49. K. Barsanti, A. Carlton and S. Chung, Analyzing experimental data and model parameters: implications for predictions of SOA using chemical transport models, *Atmos. Chem. Phys.*, 2013, **13**, 12073-12088.

View Article Online
DOI: 10.1039/C8EM00144H



50. L. Hong, U. Ghosh, T. Mahajan, R. Zare and R. Luthy, PAH sorption mechanism and partitioning behavior in lampblack-impacted soils from former oil-gas plant sites, *Environ. Sci. Technol.*, 2003, **37**, 3625-3634.

51. R. Simo, J. Grimalt and J. Albaiges, Loss of unburned-fuel hydrocarbons from combustion aerosols during atmospheric transport, *Environ. Sci. Technol.*, 1997, **31**, 2697-2700.

52. N. Zhang, Y. Yang, Y. Liu and S. Tao, Determination of octanol-air partition coefficients and supercooled liquid vapor pressures of organochlorine pesticides, *J. Environ. Sci. Heal. B*, 2009, **44**, 649-656.

53. C. Wei, Y. Han, B. Bandowe, J. Cao, R. Huang, H. Ni, J. Tian and W. Wilcke, Occurrence, gas/particle partitioning and carcinogenic risk of polycyclic aromatic hydrocarbons and their oxygen and nitrogen containing derivatives in Xi'an, central China, *Sci. Total Environ.*, 2015, **505**, 814-822.

54. J. Cao, S. Lee, K. Ho, X. Zhang, S. Zou, K. Fung, J. Chow and J. Watson, Characteristics of carbonaceous aerosol in Pearl River Delta Region, China during 2001 winter period, *Atmos. Environ.*, 2003, **37**, 1451-1460.

55. N. Kwamena, M. Staikova, D. Donaldson, I. George and J. Abbatt, Role of the aerosol substrate in the heterogeneous ozonation reactions of surface-bound PAHs, *J. Phys. Chem. A*, 2007, **111**, 11050-11058.

56. M. Riva, R. Healy, P. Flaud, E. Perraudin, J. Wenger and E. Villenave, Kinetics of the Gas-Phase Reactions of Chlorine Atoms with Naphthalene, Acenaphthene, and Acenaphthylene, *J. Phys. Chem. A*, 2014, **118**, 3535-3540.

57. J. Grossman, A. Stern, M. Kirich and T. Kahan, Anthracene and pyrene photolysis kinetics in aqueous, organic, and mixed aqueous-organic phases, *Atmos. Environ.*, 2016, **128**, 158-164.

58. M. Scalley and D. Baker, Protein folding kinetics exhibit an Arrhenius temperature dependence when corrected for the temperature dependence of protein stability, *Proc. Natl. Acad. Sci. U. S. A.*, 1997, **94**, 10636-10640.

59. Y. Sekine, H. Imanaka, T. Matsui, B. Khare, E. Bakes, C. Mckay and S. Sugita,

View Article Online
DOI: 10.1039/C8EM00144H



The role of organic haze in Titan's atmospheric chemistry I. Laboratory investigation on heterogeneous reaction of atomic hydrogen with Titan tholin, *Icarus*, 2008, **194**, 186-200.

60. M. Calisto, P. Verronen, E. Rozanov and T. Peter, Influence of a Carrington-like event on the atmospheric chemistry, temperature and dynamics, *Atmos. Chem. Phys.*, 2012, **12**, 8679-8686.
61. F. Canonaco, J. Slowik, U. Baltensperger and A. Prevot, Seasonal differences in oxygenated organic aerosol composition: implications for emissions sources and factor analysis, *Atmos. Chem. Phys.*, 2015, **15**, 6993-7002.
62. X. Wang, Z. Shen, J. Cao, L. Zhang, L. Liu, J. Li, S. Liu and Y. Sun, Characteristics of surface ozone at an urban site of Xi'an in Northwest China, *J. Environ. Monit.*, 2012, **14**, 116-126.
63. X. Ren, W. Brune, A. Oliger, A. Metcalf, J. Simpas, T. Shirley, J. Schwab, C. Bai, U. Roychowdhury, Y. Li, C. Cai, K. Demerjian, Y. He, X. Zhou, H. Gao and J. Hou, OH, HO2, and OH reactivity during the PMTACS-NY Whiteface Mountain 2002 campaign: Observations and model comparison, *J. Geophys. Res.-Atmos.*, 2006, **111**.
64. D. Vione, V. Maurino, C. Minero, E. Pelizzetti, M. Harrison, R. Olariu and C. Arsene, Photochemical reactions in the tropospheric aqueous phase and on particulate matter, *Chem. Soc. Rev.*, 2006, **35**, 441-453.
65. R. Cheung, K. Li, S. Wang, T. Pongetti, R. Cageao, S. Sander and Y. Yung, Atmospheric hydroxyl radical (OH) abundances from ground-based ultraviolet solar spectra: an improved retrieval method, *Appl. Optics*, 2008, **47**, 6277-6284.
66. R. Lohmann and G. Lammel, Adsorptive and absorptive contributions to the gas-particle partitioning of polycyclic aromatic hydrocarbons: State of knowledge and recommended parametrization for modeling, *Environ. Sci. Technol.*, 2004, **38**, 3793-3803.
67. B. Mmereki, S. Chaudhuri and D. Donaldson, Enhanced uptake of PAHs by organic-coated aqueous surfaces, *J. Phys. Chem. A*, 2003, **107**, 2264-2269.

View Article Online
DOI: 10.1039/C8EM00144H